

# Chapter 2

## Cellulosic Polymer Blends 1: With Vinyl Polymers

Kazuki Sugimura and Yoshiyuki Nishio

**Abstract** This chapter reviews recent studies on blends of conventional cellulose esters (CEs), such as cellulose acetate (CA), cellulose propionate (CP), and cellulose butyrate (CB), with non-crystalline vinyl (co)polymers mainly comprising the *N*-vinyl pyrrolidone (VP) unit. The mixing behavior of the CE/VP-containing copolymer blends is seriously affected by the chain length (i.e., carbon number) and degree of substitution (DS) as to the acyl substituent of the CE component, and by the VP fraction in the copolymer component. Relatively low-substituted CEs are commonly miscible with VP-containing copolymers by virtue of hydrogen bond formation between the CE-hydroxyls and VP-carbonyls. The blend systems using CP and CB with higher DSs impart a “miscibility window” involved in the monomer composition that constitutes the copolymer component. This observation is interpretable as a result of the indirect CE–copolymer attraction driven by intra-copolymer repulsion. A convincing argument for the miscibility behavior is provided by assessing the attractive or repulsive interactions between the blend constituents in terms of the viscometric interaction parameter. In addition to the basic characterization of the blend miscibility and intermolecular interaction, we also survey some useful applications of miscible CE blends to functional films exhibiting improved adsorption, optical, or thermomechanical properties. Particular attention is paid to the molecular orientation and optical anisotropy induced in deformed films of CA/VP-methyl methacrylate polymer blends.

**Keywords** Blends • Cellulose ester • Interaction • Miscibility • Miscibility window • Optical films • Scale of homogeneity • Vinyl copolymer • *N*-Vinyl pyrrolidone • Viscometric interaction parameter

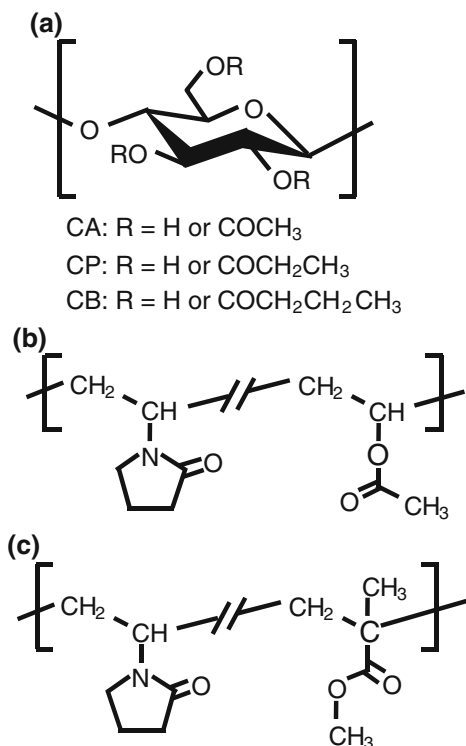
### 2.1 Introduction

Cellulose and its derivatives have been commercially available for nearly a century. Among the derivatives, organic esters of cellulose (CEs) are industrially important materials; they are utilized as packaging, coatings, excipients, molded plastics,

fibers, optical films, and membranes and other separation media [1, 2]. Toward enhancing the consumption of CEs for conventional use and exploiting of new CE applications, improving or variegating their physical properties is desired to satisfy diverse requests for future use. Graft copolymerization or polymer blending of CEs can be a promising approach to this end [1, 3–5]. In any of the two techniques, the molecular-scale mixing with an appropriate second polymer component would offer an opportunity to design new polymeric materials that exhibit wide-ranging and/or synergistic functions unattainable in gross mechanical mixtures and single-component materials. In particular, miscible blending of two polymers may be practically useful to alter the original physical properties and functions of CEs at the lowest possible cost.

In reality, two different polymers rarely form a homogeneous blend, because there is little or no contribution of the combinatorial entropy of mixing to the attainment of miscibility in polymer blends [6–9]. It is still difficult to precisely predict which polymer pair will form a miscible phase. At least, however, an attractive force, such as hydrogen bonding, dipole–dipole interaction, or ionic interaction, should be required to realize the polymer–polymer miscibility, as is described in Chap. 1. In the case of cellulosic blends, residual hydroxyl groups on the glucopyranose unit can offer the specific intercomponent interactions.

**Fig. 2.1** Structural formulae of **a** representative CEs, i.e., CA, CP, and CB, **b** P(VP-*co*-VAc), and **c** P(VP-*co*-MMA)



Concerning polymer blends of CEs, the authors' group has conducted a sequence of fundamental and practical studies for more than a decade using cellulose acetate (CA), propionate (CP), and butyrate (CB) as representative CEs (Fig. 2.1a). The counter components examined so far are categorized as two main types of polymers: biodegradable aliphatic polyesters [e.g., poly(3-hydroxybutyrate) and poly( $\epsilon$ -caprolactone)] and synthetic vinyl polymers. The former polymer blends are designed for biodegradable plastics, and the results will be summarized in Chap. 3. The present chapter covers work on binary blends of CEs with non-crystalline vinyl polymers. A comparative investigation of the miscibility and intermolecular interaction is summarized systematically for several systems of CE/vinyl polymer blends. Application of the miscible blends to functional optical films and membranes is also exemplified. Besides these, some related work aimed at enhancing the mechanical performance of CE blends is briefly reviewed.

## 2.2 Cellulose Ester Blends with *N*-Vinyl Pyrrolidone Copolymer

Cellulose acetate CA is a particularly important cellulose ester and utilized for many applications due to its desirable physical properties such as good optical clarity in film form, and a comparatively high modulus and adequate flexural and tensile strengths in fiber form. However, a trouble is that CA alone cannot be molded so easily by thermal processing, because its glass transition temperature ( $T_g$ ) and melting point are fairly high, where significant thermal decomposition can take place. Therefore, in practice, a large amount of plasticizer (e.g., phthalate compound) is usually mixed with CA for the thermal molding. The use of low molecular-weight plasticizers, however, can cause fume generation in the molding process due to their volatility or decomposition. In addition, bleeding-out of plasticizers from molded CA products can be pronounced in long-term uses. Accordingly, it is of great significance to improve the original thermal property of CA by incorporation with flexible polymers as plasticizer through molecular-level interactions.

Taking into account the hydrogen-bonding formability of cellulosics, a blending partner of CEs including CA would be desired to have a proton-accepting capacity. One of the suitable polymers is poly(*N*-vinyl pyrrolidone) (PVP); in fact, it has been shown that PVP can form compatible blends with unmodified cellulose [10, 11]. Since PVP and its copolymers are widely prevailing in medical, sanitary, cosmetic, and other safety-conscious areas, the selection of vinyl copolymers containing an *N*-vinyl pyrrolidone (VP) unit (Fig. 2.1b, c) is promising for improvement in properties of the CE family. Actually, CEs are also usable in bio-related fields, e.g., as separation membranes and release-controllable excipients. The miscible incorporation with the VP-containing polymers may be expected to improve the thermal,

gas permeation, and water absorption properties of CEs, and possibly provides another excellent functionality unrealized by CEs themselves; the latter effect is really found in an optical function for film use (Sect. 2.2.3).

### 2.2.1 Miscibility Maps as a Function of DS and Copolymer Composition

#### (a) Cellulose Ester/Poly(*N*-vinyl pyrrolidone-co-vinyl acetate) Blends

Miyashita et al. carried out the miscibility characterization of CA blends with homo- and random co-polymers comprising VP and/or vinyl acetate (VAc) units, i.e., PVP, poly(vinyl acetate) (PVAc), and poly(*N*-vinyl pyrrolidone-co-vinyl acetate) (P(VP-co-VAc)) (Fig. 2.1b) [12]. The CA/synthetic polymer blends were all prepared in film form by casting from mixed polymer solutions in *N,N*-dimethylformamide (DMF) or *N,N*-dimethylacetamide. On the basis of thermal transition data obtained by differential scanning calorimetry (DSC), a miscibility map (Fig. 2.2a) was completed as a function of the degree of substitution (DS) of CA and the VP fraction in P(VP-co-VAc). Figure 2.3 exemplifies a result of the DSC measurements for two blending pairs of CA/P(VP-co-VAc) corresponding to the polymer combinations marked as **A** and **B** in Fig. 2.2a; the miscibility was estimated by  $T_g$  criteria (see Sect. 1.3.1 of Chap. 1), after heat treatment of the samples above  $T_g$  of both components to equalize their thermal history. In the DSC data (Fig. 2.3a) for the blends of CA (DS = 2.95) with P(VP-co-VAc) of VP = 61 mol% (combination **A**), we can readily see a sign of poor miscibility, as is evidenced from no appreciable shift in the  $T_g$ s of both polymer components. In addition to the two distinguishable  $T_g$  signals, the melting endotherm and cold-crystallization exotherm of the CA component are both detectable for every blend at almost the same temperature positions as those for the triacetate alone. In contrast to this result, the thermograms collected in Fig. 2.3b for the pair of CA (DS = 2.70) and the same P(VP-co-VAc) (VP = 61 mol%) (combination **B**) show a miscible behavior, as indicated by a single  $T_g$  that shifts to the higher temperature side along with the increase in the CA content.

As summarized in Fig. 2.2a, the miscibility behavior of the CA/P(VP-co-VAc) series is found to be significantly affected by both the DS of CA and the copolymer composition. FT-IR and solid-state  $^{13}\text{C}$  NMR spectroscopic measurements revealed the presence of hydrogen-bonding interactions formed between CA-hydroxyls and VP-carbonyls in the miscible blends, which was evidenced by observations of a systematic peak shift for the relevant signals of IR bands and carbon resonances [12, 13]. The role of intermolecular hydrogen-bondings in the CA-vinyl polymer miscibility was made more explicit through a pseudo complexation behavior from solutions in a poor solvent [13]. When CA and P(VP-co-VAc) solutions in tetrahydrofuran were mixed with each other, the two polymer components precipitated spontaneously to form a complex-like agglomerate, due to stronger

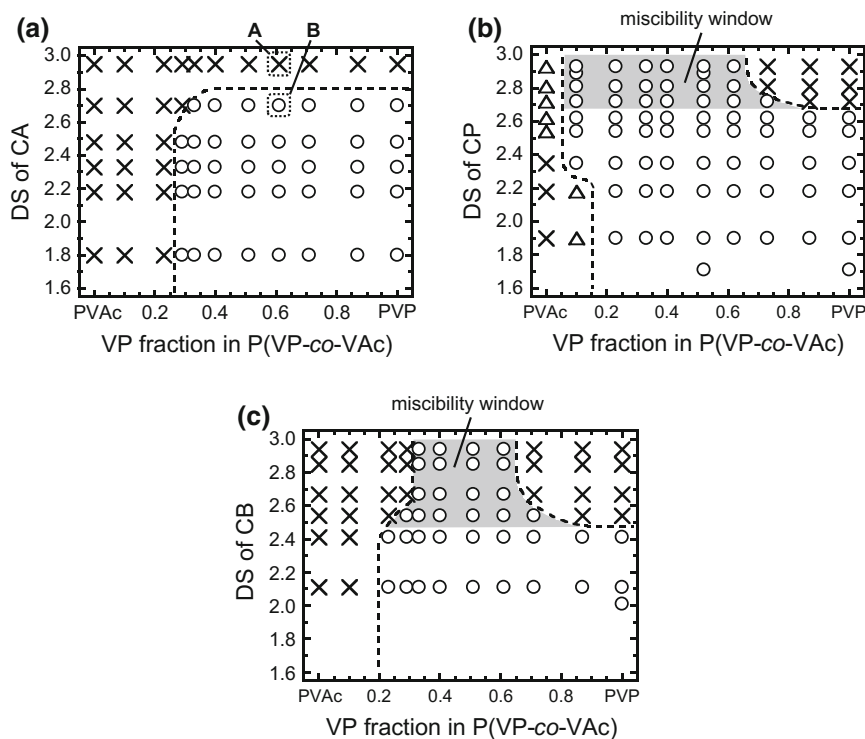


**Fig. 2.2** Miscibility maps for three blend systems: **a** CA/P(VP-*co*-VAc), **b** CP/P(VP-*co*-VAc), and **c** CB/P(VP-*co*-VAc), depicted as a function of DS of CE and VP fraction in the vinyl copolymer. Symbols indicate that a given pair of CE/P(VP-*co*-VAc) is miscible (open circle, single  $T_g$ ), immiscible (cross, dual  $T_g$ s), or partially miscible (open triangle, dual  $T_g$ s approaching each other to an appreciable degree) [Quoted with permission from [12] for (a), [14] for (b), and [15] for (c)]

attraction between the pair polymers in preference to their respective solvations. The yield of the precipitate diminished with increasing DS of CA, viz., decreasing residual hydroxyl groups on the glucopyranose residues, and with decreasing VP fraction in the vinyl copolymer. The  $T_g$  value of the complexes was always higher than that of blend films cast from solutions in DMF as good solvent. This observation suggests that a high frequency of interactions combines CA with vinyl polymers intimately in their complex to seriously reduce the mobilities of the individual polymer chains.

In a similar manner to that for the CA/P(VP-*co*-VAc) system, the miscibility state in the blends of cellulose propionate (CP) [14] and butyrate (CB) [15] with P(VP-*co*-VAc) was estimated by  $T_g$  determination with DSC. The results for the two systems are summarized in Fig. 2.2b, c, respectively, by constructing the corresponding miscibility maps. Compared to the previous map of the CA series (Fig. 2.2a), the critical DS required for attainment of the miscibility of CP and CB with PVP homopolymer is appreciably lower ( $\sim 2.65$  for CP;  $\sim 2.5$  for CB). This is

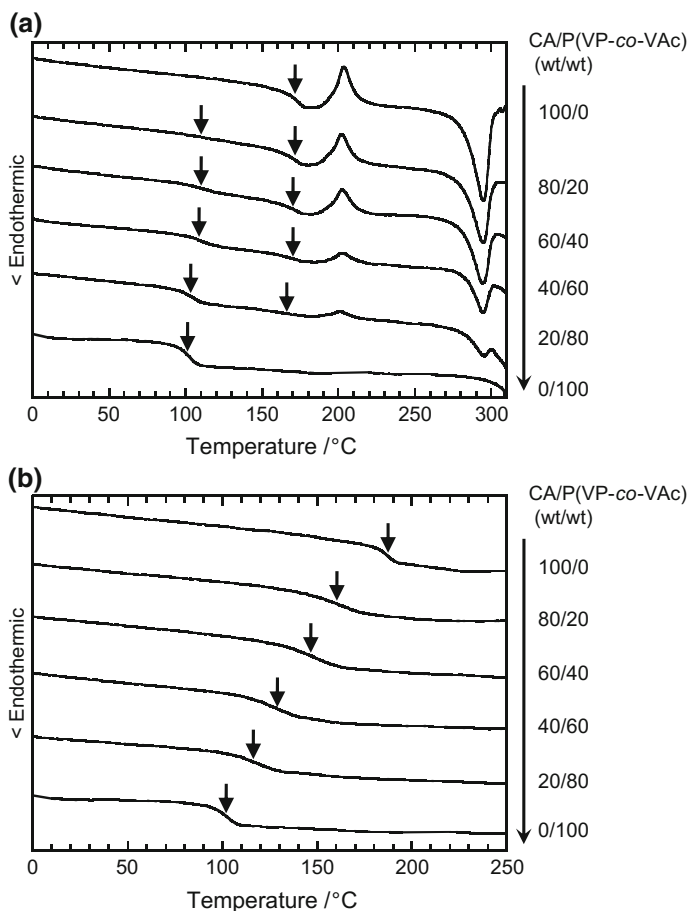


**Fig. 2.3** DSC thermograms of CA/P(VP-*co*-VAc) blends: **a** data for combination **A** of CA (DS = 2.95) and P(VP-*co*-VAc) (VP:VAc = 61:39); **b** data for combination **B** of CA (DS = 2.70) and P(VP-*co*-VAc) (VP:VAc = 61:39) (see Fig. 2.2a). Arrows indicate a  $T_g$  position taken as the midpoint of a baseline shift in heat flow

because the intermolecular hydrogen-bonding interaction, as a driving force for the CE–PVP miscibility, is suppressed in frequency by steric hindrance of the comparatively bulky substituent (propionyl or butyryl side-group).

Unlike the situation in the CA series, high-substituted CPs (DS > 2.65) and CBs (DS > 2.5) make a miscible pair with some of the copolymers (not rich in VP) in spite of their immiscibility with both PVP and PVAc homopolymers (see Fig. 2.2b, c). This unique miscibility behavior, i.e., advent of a “miscibility window,” is attributed to an indirect CE–copolymer attraction that is driven by repulsion between the two monomeric units constituting the vinyl copolymer. More concretely, since these two monomer species, VP and VAc, having mutually repellent characters were randomly

combined in P(VP-*co*-VAc) by covalent bonding, the copolymers can form a miscible monophase with the CE component in the binary blends so as to reduce the strong repulsion between the comonomers. Such an explicit window never appears in the CA/P(VP-*co*-VAc) map (Fig. 2.2a). This may be interpreted as due to a stronger self-association ability of CA, which becomes pronounced when the DS exceeds  $\sim 2.75$ ; the CA rather crystallizes in a cellulose triacetate II form (see Fig. 2.3a). Differing from this, no crystallizing habit is detected even for tripropionate and tributyrates samples synthesized at DS = 2.8–2.95. The lesser self-association nature of CP and CB should be advantageous to the indirect attractive interaction with the P(VP-*co*-VAc) component.

From comparison of the three maps shown in Fig. 2.2, it is astonishing afresh to find that only one difference in carbon number of the acyl substitution drastically changes the region of miscible CE/P(VP-*co*-VAc) pairings. Intriguingly, the CP system (Fig. 2.2b) provides the largest miscible region. In particular, it should be stressed that the high-substituted CPs of DS > 2.7 are miscible with P(VP-*co*-VAc) s abundant in VAc residue. At the VAc-richer compositions, the intramolecular repulsion effect in P(VP-*co*-VAc) would decline to a considerable extent. Instead, a weak interaction coming from the structural affinity between the propionyl and VAc moieties (see below) would contribute as another driving force. This is supported by  $T_g$  behavior of CP/PVAc pairs. Figure 2.4 collects  $T_g$  versus composition plots for five series of CP/PVAc blends (propionyl DS = 2.18–2.93). The blend series using CPs of DS = 2.18 and 2.35 are completely immiscible. Regarding the other blend series using CPs of DS > 2.5, however, an appreciable extent of  $T_g$  shift is

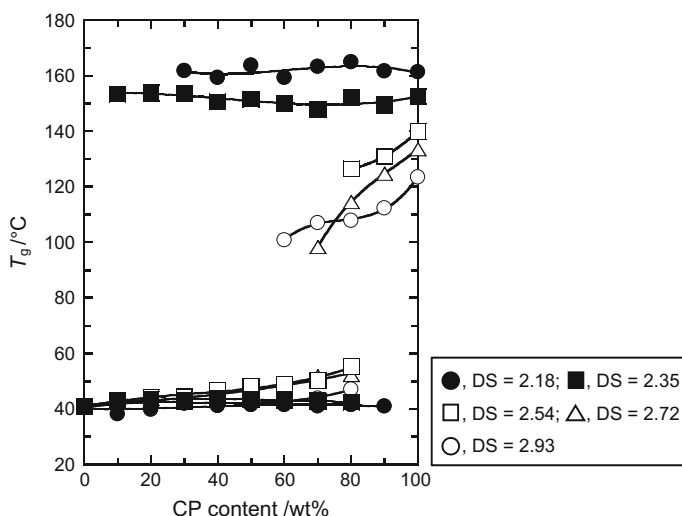


**Fig. 2.4**  $T_g$  versus composition plots for five series of CP/PVAc blends. DS of CP: filled circle, 2.18; filled square, 2.35; open square, 2.54; open triangle, 2.72; open circle, 2.93. (Quoted with permission from [14])

detected for both of the two components at compositions of CP/PVAc = 60/40–90/10 (wt/wt). This observation indicates that a certain amount of the CP constituent is dissolved into the PVAc phase, and vice versa. Therefore, we can judge the CP ( $DS > 2.5$ )/PVAc pairs to be partially miscible. Such partial miscibility was never definable to the CA/PVAc and CB/PVAc systems irrespective of DS of the CA and CB components; the two systems always provided two invariable  $T_g$ s independent of the mixing composition. The structural affinity between the propionyl side-group ( $\text{CH}_3\text{-CH}_2\text{-CO-O-C-}$ ) and the VAc unit ( $\text{-(CH}_2\text{-CH(-O-CO-CH}_3\text{))-}$ ) is favorable for an interaction of dipole–dipole antiparallel alignment, which might be responsible to that partial miscibility (or better compatibility).

### (b) *Cellulose Ester/Poly(N-vinyl pyrrolidone-co-methyl methacrylate) Blends*

Similar representations of the miscibility estimation based on DSC thermal analysis are given in Fig. 2.5 for two systems; a random copolymer comprising VP and methyl methacrylate (MMA) units, P(VP-co-MMA) (Fig. 2.1c), is combined with either CA (Fig. 2.5a) [16] or CP (Fig. 2.5b) [17]. The mapping for CB/P(VP-co-MMA) blends is not made in the figure, because  $T_g$ s (ca. 110–120 °C) of CBs of  $DS \approx 2.5\text{--}2.9$  were too close to those (ca. 100–115 °C) of P(VP-co-MMA)s of VP < 50 mol%. The incorporation of MMA into the vinyl polymer as a counterpart of the CE blends may be practically significant, for poly(methyl methacrylate) (PMMA) is important as optical and medical materials based on its distinguished performance and safety to living bodies.

As can be seen from the map shown in Fig. 2.5a, most of the pairs composed of CA of  $DS \leq 2.6$  and P(VP-co-MMA) of VP  $\geq \sim 30$  mol% are miscible, whereas the other combinations of DS and VP values basically lead to an immiscible blend series. The driving factor for the miscibility attainment was ascertained to be the hydrogen-bonding formed between the CA-hydroxyls and the VP-carbonyls [16], as in the case of the CA/P(VP-co-VAc) system. As for CA/PMMA homopolymer blends, two independent glass transitions associated with the two components were discernible irrespective of DS of the CA used, but the  $T_g$  of the PMMA component slightly shifted to higher temperatures with increasing CA content. This suggests that PMMA shows a limited degree of miscibility with CA [16, 18]; however, the  $T_g$  of the CA component hardly shifted from the original position. Thus the CA/PMMA pairs were all judged to be substantially immiscible.

Compared to the CA system, the miscible pairing region in the CP/P(VP-co-MMA) map (Fig. 2.5b) expands to cover a considerably hydrophobic area of higher DS and MMA-rich composition [17]. The appearance of a miscible region of propionyl  $DS \leq 2.65$  and VP  $\geq \sim 10$  mol% owes to the intercomponent hydrogen-bondings. In the upper region satisfying  $DS > 2.7$  and VP = ca. 10–40 mol%, a clear miscibility window emerges as a result of the indirect attraction due to intramolecular repulsion in the P(VP-co-MMA) component. The location of the window in the side of MMA-rich compositions would owe to better affinity between propionyl and MMA moieties, which was supported by the composition-dependent shift of PMMA's  $T_g$  observed for a blend series of CP/PMMA. In comparison between the two maps shown in Figs. 2.2b and 2.5b,



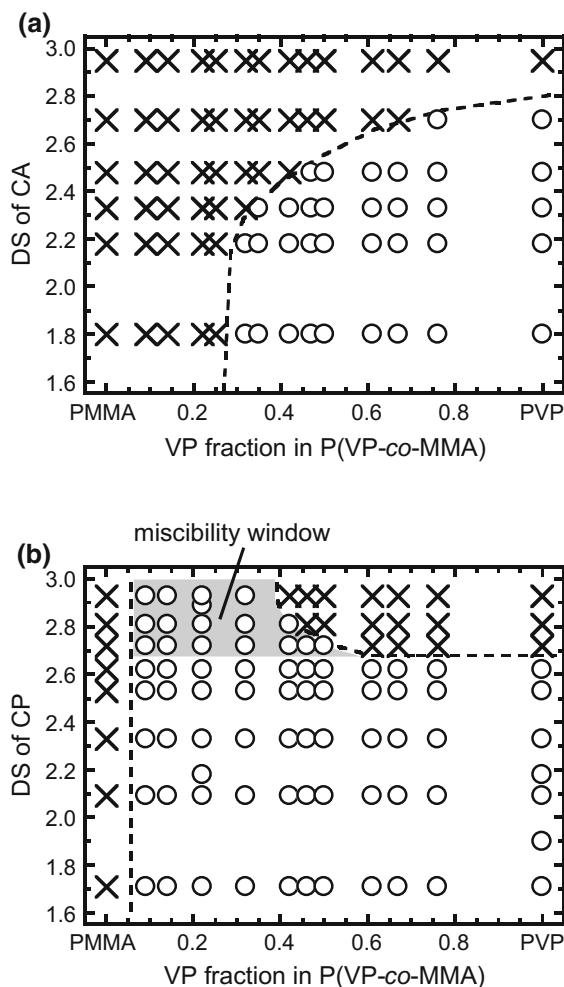


**Fig. 2.5** Miscibility maps for two blend systems: **a** CA/P(VP-co-MMA) and **b** CP/P(VP-co-MMA), depicted as a function of DS of CE and VP fraction in the vinyl copolymer. The meanings of two symbols *open circle* and *cross* are the same as defined in Fig. 2.2. [Quoted with permission from [16] for (a) and [17] for (b)]

obviously, the window region for the CP/P(VP-co-MMA) system is narrower than that for the CP/P(VP-co-VAc) system. This narrowing might be ascribed to the weaker repulsion between VP and MMA units relative to that in the VP-VAc copolymer. In this connection, the contribution of such an intra-copolymer effect is made clearer from estimation of certain interaction parameters associated with the two copolymers (see Sect. 2.2.2). To make another comparison involving CA blends, the miscible region in the CA/P(VP-co-MMA) map (Fig. 2.5a) is also narrower than that in the CA/P(VP-co-VAc) map (Fig. 2.2a). This implies that the

intra-copolymer effect is present latently in the CA/vinyl polymer blends, although the hydrogen-bonding interaction predominantly works to realize the respective blend miscibility.

(c) *Cellulose Mixed Ester Blends with N-Vinyl Pyrrolidone Copolymer*

From the above comparative study, it is evident that the miscibility behavior of CEs (i.e., CA, CP, and CB) with VP-containing vinyl copolymer, P(VP-co-VAc) or P(VP-co-MMA), is largely affected by a small difference in alkyl chain-length (carbon number) of the acyl substituent in the employed CE. As an expansion of the blend series using the monoester derivatives of cellulose, additional attention has been directed to the miscibility behavior of binary blends of cellulose mixed ester with the VP-containing copolymers. Traditional mixed esters, cellulose acetate propionate (CAP) and acetate butyrate (CAB), are employed here as the cellulosic component.

Figure 2.6 shows an estimation result of the blend miscibility of four different CABs (#1–4) with P(VP-co-VAc) [15]; the total DS of CAB used ranges from 2.4 to 2.7. CAB#1 and #2 are acetyl-rich and butyryl-rich CAB samples, respectively, and the two contain appreciable amounts of both acetyl and butyryl groups. CAB#3 and #4 are butyryl-rich CABs of total DS = 2.68 and 2.39, respectively. With regard to the CAB#3 and #4, their behavior of miscibility with the vinyl polymer (lower two data in Fig. 2.6) resembles that of CBs having comparable DSs in the total substitution (see Fig. 2.2c). The others, CAB#1 and #2, are miscible with P(VP-co-VAc) in a wider range of VP:VAc composition (upper two data in Fig. 2.6), when compared with the corresponding data for CA (Fig. 2.2a) and CB (Fig. 2.2c) of the same degree of acyl substitution as the total DS of the CAB considered. For instance, the blend series of CAB#2 (total DS = 2.55; acetyl:butyryl = 0.96:1.59) with P(VP-co-VAc) exhibits a miscibility window, as did the corresponding series of CB (DS = 2.54), but the window observed for the former is much wider than that for the latter. This expansion of the miscible range in the copolymer composition may be interpreted as due to an additional repulsion effect originating in the CAB component. That is, the cellulose mixed ester would also

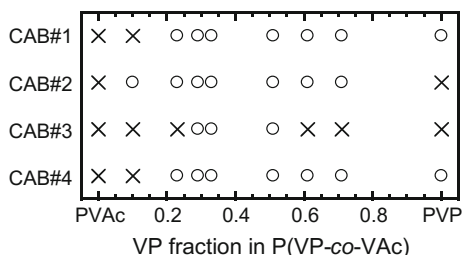


**Fig. 2.6** Miscibility estimation for CAB/P(VP-co-VAc) blend series using four CABs: CAB#1 of total DS = 2.71 and acetyl:butyryl = 2.00:0.71; CAB#2 of total DS = 2.55 and acetyl:butyryl = 0.96:1.59; CAB#3 of total DS = 2.68 and acetyl:butyryl = 0.14:2.54; CAB#4 of total DS = 2.39 and acetyl:butyryl = 0.14:2.25. The meanings of two symbols *open circle* and *cross* are the same as defined in Fig. 2.2 (Rearranged by using data from [15], with permission)

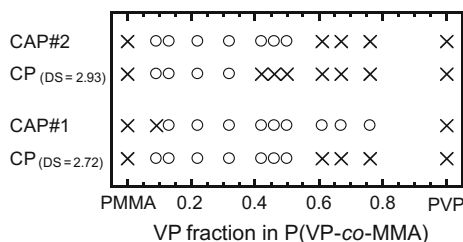


**Fig. 2.7** Miscibility estimation for CAP/P(VP-*co*-MMA) blends using two CAPs (CAP#1, total DS = 2.68 and acetyl:propionyl = 0.16:2.52; CAP#2, total DS = 2.95 and acetyl:propionyl = 0.47:2.48), in comparison with the corresponding CP/P(VP-*co*-MMA) blends using CPs of DS = 2.72 and 2.93 (see Fig. 2.5b), respectively. The meanings of two symbols *open circle* and *cross* are the same as defined in Fig. 2.2 (Quoted with permission from [17])

behave as a kind of copolymer dangling two different acyl side-groups along the carbohydrate backbone. Therefore, the CAB/P(VP-*co*-VAc) system is actually taken as a copolymer/copolymer system, where the miscibility should be affected by the duplicate, intramolecular copolymer effect.

A similar deal of cellulose mixed ester as copolymer is applicable to another system of CAP/P(VP-*co*-MMA) [17]. Figure 2.7 summarizes the miscibility estimation for the two CAP/P(VP-*co*-MMA) series using CAP#1 (total DS = 2.68; acetyl:propionyl = 0.16:2.52) and CAP#2 (total DS = 2.95; acetyl:propionyl = 0.47:2.48). The corresponding data for comparable CP/P(VP-*co*-MMA) blends using CPs of DS = 2.72 and 2.93 are also shown in the figure. Owing to the additional repulsion effect originating in the CAP side, both the CAP series offer a miscibility window over a wider range of the VP:MMA copolymer composition, compared to the CP series of the corresponding DS in total.

The dual acylation leading to a mixed ester of cellulose is practically useful to improve the blend miscibility (or compatibility) with a second polymer as plasticizer. For instance, as the demonstration is described in Chap. 5, we can design a compatible system of cellulose mixed ester/flexible polymer showing an adequate melt-spinnability; thereby it will become possible to create a new type of cellulosic fiber by melt spinning.

## 2.2.2 Intermolecular Interaction and Homogeneity Scale

### (a) Polymer-Polymer Interaction Parameter Determined by Viscometry

As described in Sect. 2.2.1, the CE/VP-containing copolymer combinations assume miscible or immiscible behavior according to the balance in effectiveness of the following four factors: (1) hydrogen-bonding attraction between residual hydroxyls of CE and VP-carbonyl groups of the vinyl copolymer; (2) steric hindrance of bulky side-groups to the interaction specified in (1); (3) indirect attraction via intramolecular repulsion between the comonomer units in the copolymer; and

(4) weak interaction due to structural affinity (e.g., dipole–dipole antiparallel alignment) between the ester side-group of CE (such as  $\text{CH}_3\text{-CH}_2\text{-CO-O-C-}$ ) and the VAc ( $\text{-(CH}_2\text{-CH(O-CO-CH}_3\text{))-}$ ) or MMA ( $\text{-(CH}_2\text{-(CH}_3\text{)C(CO-O-CH}_3\text{))-}$ ) unit. Probably by virtue of the factors 3 and 4, the blend miscibility of CP with the VP-containing vinyl copolymer is more improved in respect of the miscible pairing number, compared to the cases using CA and CB. However, these two factors could not be directly detected by spectroscopic measurements.

To clarify the contributions of the copolymer effect and structural affinity to the miscibility attainment, attractive or repulsive interactivity between the CE and vinyl polymer constituents was quantitatively discussed in terms of polymer–polymer interaction parameters determinable by dilute solution viscometry [16, 19]. In the viscometric treatment developed by Krigbaum and Wall [20] and other groups [21, 22], the polymer–polymer miscibility can be estimated by comparison between an experimentally obtained value and an ideally calculated one of viscometric interaction parameter for dilute blend solution, i.e.,  $b_m^{\text{ex}}$  and  $b_m^{\text{id}}$ , respectively. When there is a large difference between the intrinsic viscosity of both polymers ( $[\eta]_1$  and  $[\eta]_2$ ), a so-called Krigbaum-Wall interaction parameter,  $\Delta b$  ( $= b_m^{\text{ex}} - b_m^{\text{id}}$ ), can be standardized, and a more effective parameter,  $\mu$ , is obtained by using the following equation [22]:

$$\mu = \frac{\Delta b}{([\eta]_2 - [\eta]_1)^2} \quad (2.1)$$

If  $\mu$  is positive, the polymer 1 and polymer 2 are mutually attractive and therefore the pair is taken as miscible. Contrarily, if  $\mu$  is negative, the repulsive pair is considered to be immiscible. The absolute value of  $\mu$ , i.e.,  $|\mu|$ , should represent the relative strength of attractive or repulsive interaction between the two component polymer molecules. In fact, the  $[\eta]$  values (2–6 dL/g) of the cellulosics and those (0.1–0.6 dL/g) of the vinyl (co)polymers are fairly far apart, and hence the standardized parameter  $\mu$  is mainly used below for discussion on the interaction and miscibility between the blend constituents.

Figure 2.8 summarizes simplified miscibility maps (left) of the three blend systems of CA, CP, CB each blended with P(VP-co-VAc), with addition of the illustration in terms of  $\mu$  data (right) obtained for selected polymer combinations (DS of CEs,  $\sim 2.7$ ; VP:VAc of copolymer,  $\sim 0.5:0.5$ ) critical to the respective systems [16, 19]. All the judgments based on  $\mu$  data are actually in accordance with the miscibility map based on DSC thermal analysis.

As for a highly propionylated CP (DS = 2.72)/P(VP-co-VAc) series (Fig. 2.8b), the immiscible combination of PVP and PVAc (judged in advance by DSC) provides a larger negative  $\mu$  value ( $-4.23 \times 10^{-2}$ ) than the CP/PVP ( $-1.02 \times 10^{-2}$ ) and CP/PVAc ( $-7.19 \times 10^{-5}$ ) pairs. A CB (DS = 2.67)/P(VP-co-VAc) series (Fig. 2.8c) also shows a similar relationship of repulsion (immiscibility) between the three ingredient polymer pairs. By support of the  $\mu$  data, it is reasonably deduced that, due to the intense repulsion between VP and VAc segments, the P(VP-co-VAc) component can mix with the CP and CB components showing less repulsion to the comonomer units instead of the copolymer–copolymer association.

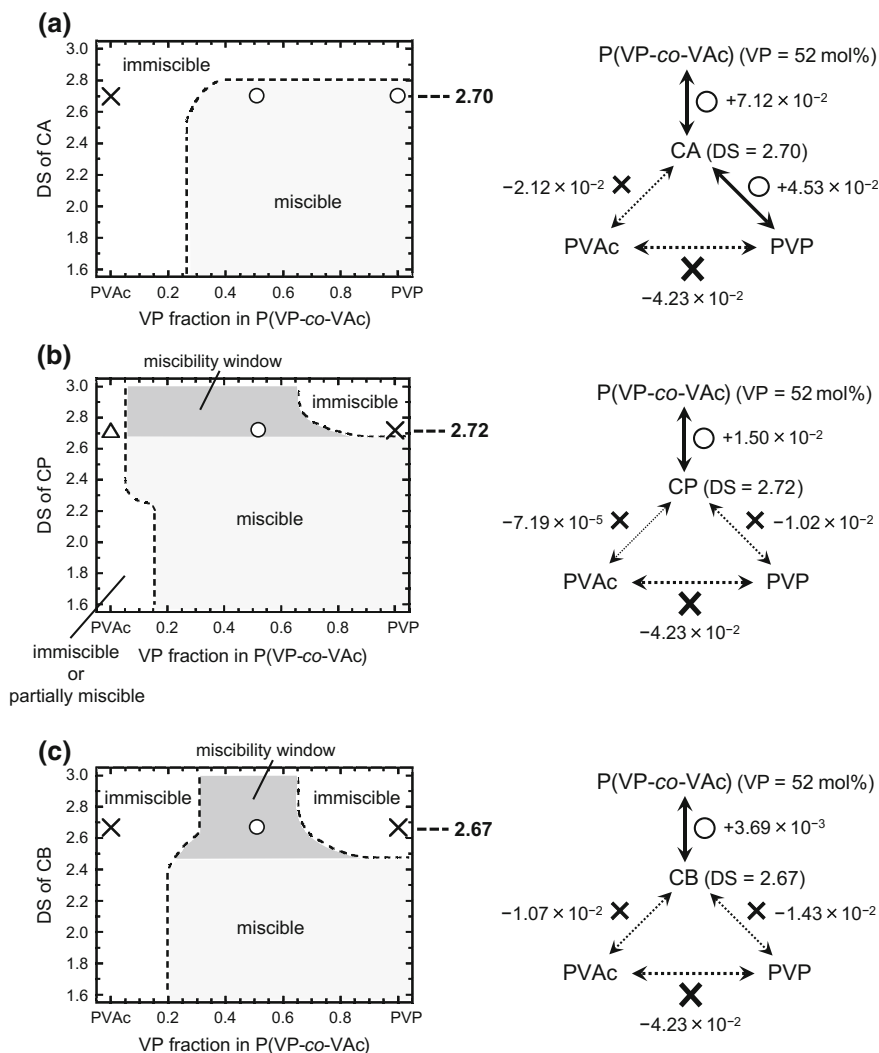


**Fig. 2.8** Miscibility maps (*left*) with additional illustrations using  $\mu$  data (*right*) for **a** CA/P(VP-co-VAc), **b** CP/P(VP-co-VAc), and **c** CB/P(VP-co-VAc) systems. The meanings of three symbols *open circle*, *cross*, and *open triangle* are the same as used in Fig. 2.2 (Quoted with permission from [19], with an adequate modification)

Another interesting observation in Fig. 2.8 is that the negative  $\mu$  value for the CP (DS = 2.72)/P(VP-co-VAc) pair is much smaller than that for the CP/PVP pair by more than two orders of magnitude. The value in  $|\mu|$ ,  $7.19 \times 10^{-5}$ , for the CP/P(VP-co-VAc) pair is also overwhelmingly small, compared with  $|\mu| = 2.12 \times 10^{-2}$  for CA (DS = 2.70)/P(VP-co-VAc) (Fig. 2.8a) and  $1.07 \times 10^{-2}$  for CB (DS = 2.67)/P(VP-co-VAc) (Fig. 2.8c). This low magnitude of  $\mu$  reflects the “partially miscibility” specified in the blends of highly

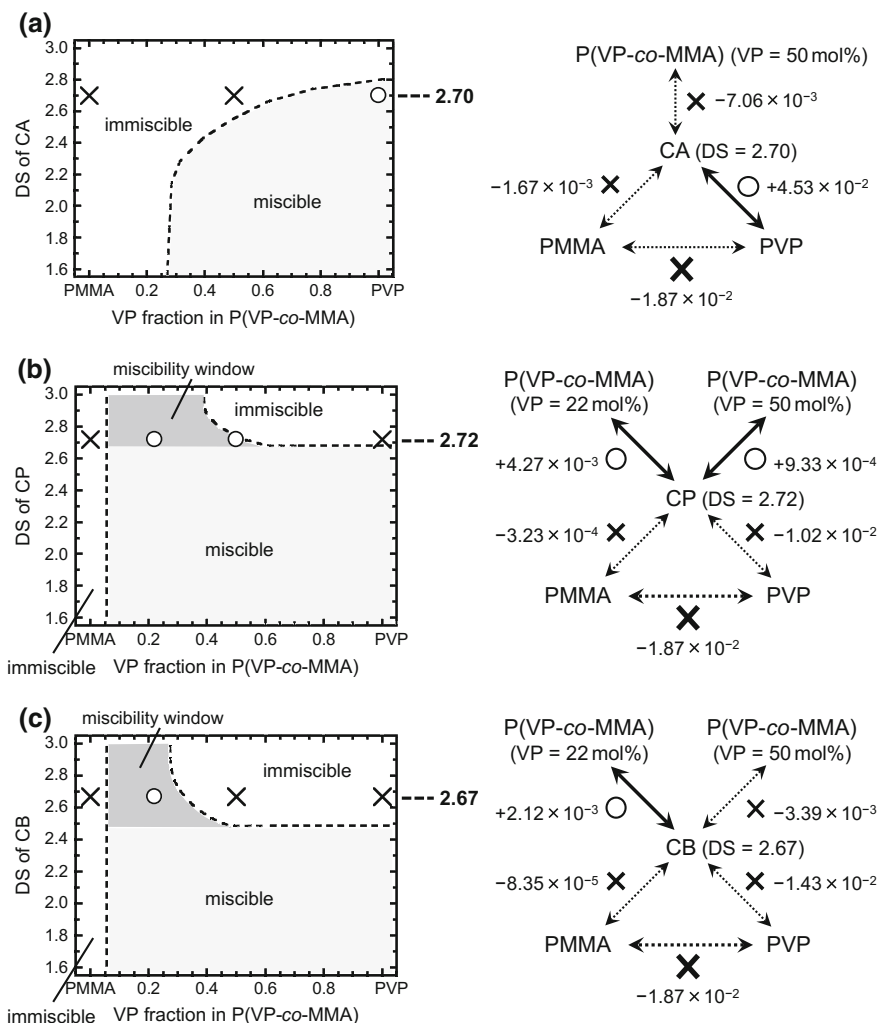


**Fig. 2.9** Miscibility maps (*left*) with additional illustrations using  $\mu$  data (*right*) for **a** CA/P(VP-co-MMA), **b** CP/P(VP-co-MMA), and **c** CB/P(VP-co-MMA) systems. The meanings of two symbols *open circle* and *cross* are the same as used in Fig. 2.2 (Rearranged by using data from [19], with permission)

substituted CPs with PVAc homopolymer (see Fig. 2.4). Such a good compatibility would lead to expansion of the miscible pairing region in the map of the CP/P(VP-co-VAc) system particularly to the side of VAc-rich compositions, in comparison with the cases using CA and CB.

As summarized in Fig. 2.9,  $\mu$  evaluations made for CA (DS = 2.70)/P(VP-co-MMA) (Fig. 2.9a) and CP (DS = 2.72)/P(VP-co-MMA) blends (Fig. 2.9b) are also in consistency with the respective miscibility mappings based on DSC analysis. The

lower order of  $\mu$  ( $10^{-3}$ – $10^{-4}$ ) obtained for the CA/PMMA and CP/PMMA pairs supports the better compatibility of the CEs with PMMA. From the triangular relationship between the three ingredient polymers participating in the CP/P(VP-*co*-MMA) series, it can be ensured that the intramolecular repulsion effect of the VP-MMA copolymer gives rise to the miscibility window in the map. However, the repulsion between the VP and MMA constituents ( $\mu = -1.87 \times 10^{-2}$ ) is weaker than the intramolecular repulsion in P(VP-*co*-VAc) ( $-4.23 \times 10^{-2}$  shown above). This deterioration of the copolymer effect is responsible for the observation of the narrower miscible region in the CE/P(VP-*co*-MMA) maps relative to that in the CE/P(VP-*co*-VAc) maps (see Fig. 2.8).

Such a useful  $\mu$  assessment may be applicable to complement the miscibility estimation for CB/P(VP-*co*-MMA) blends; the total mapping for this system has not been accomplished by DSC only. In Fig. 2.9c, a convincing map is constructed with the aid of  $\mu$  data for the system concerned. Definitely, there appears a miscibility window in the map. The miscible range of VP:MMA composition in this window is a little bit narrow, compared with the corresponding range in the CP/P(VP-*co*-MMA) map (Fig. 2.9b).

In Fig. 2.10, the miscibility estimation for CAP#1 (total DS = 2.68; acetyl:propionyl = 0.16:2.52)/P(VP-*co*-MMA) blends is inspected in  $\mu$  terms. For example, a combination of CAP#1 with P(VP-*co*-MMA) (VP = 50 mol%) provided a positive  $\mu$  data of  $+5.79 \times 10^{-3}$ , surely supporting the situation of the polymer pair in the miscibility window of the map. Furthermore, we notice that this  $\mu$  value is considerably larger than  $\mu = +9.33 \times 10^{-4}$  obtained for a comparable pair of CP (DS = 2.72)/P(VP-*co*-MMA) (VP = 50 mol%) (see Fig. 2.9b). As listed in Fig. 2.10 (right), a cellulose ester pair, CA (DS = 2.70)/CP (DS = 2.72), gave a negative  $\mu$  of  $-8.12 \times 10^{-3}$ , suggesting that a relatively strong repulsive interactivity works between the two cellulosic monoester components. From these evidences in  $\mu$  terms, it is reasonably concluded that the additional intramolecular repulsion in the CAP side contributes to the expansion of the miscibility window in the mapping of the CAP#1/P(VP-*co*-MMA) blends.

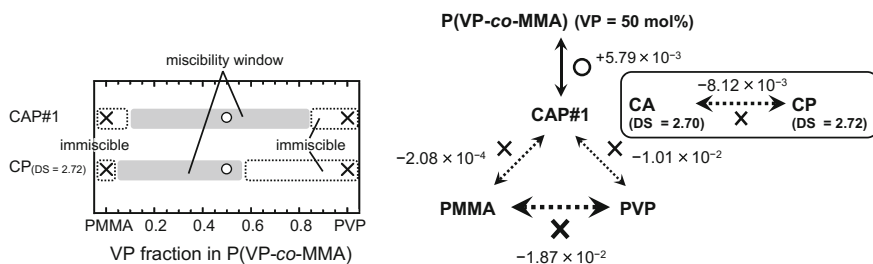


**Fig. 2.10** Miscibility estimation (left) with additional illustrations using  $\mu$  data (right) for binary polymer blends, CAP#1 (total DS = 2.68; acetyl:propionyl = 0.16:2.52)/P(VP-*co*-MMA) and CP (DS = 2.72)/P(VP-*co*-MMA). The meanings of two symbols open circle and cross are the same as used in Fig. 2.2 (Rearranged by using data from [19], with permission)

### (b) *Scale of Homogeneous Mixing*

Physical properties of polymer blends would be greatly influenced by a level of mixing. It is therefore meaningful to quantify a scale of homogeneity in even the blends judged to be miscible. In the CE/VP-containing vinyl (co)polymer blends described thus far, the principal driving force for the miscibility attainment was the intercomponent hydrogen-bonding or the intra-copolymer repulsion. The difference in effectiveness between the driving factors should affect the size of heterogeneity ( $L$ ) in the miscible blends.

As mentioned in Chap. 1, through measurements of the proton spin-lattice relaxation time in the rotating frame ( $T_{1\rho}^H$ ) by solid-state  $^{13}\text{C}$  NMR, we can estimate the mixing homogeneity in a scale of  $^1\text{H}$  spin-diffusion length ( $= 2\text{--}5\text{ nm}$ ) [23–25]; this dimensional scale is much smaller than that ( $\sim 25\text{ nm}$ ) detected by DSC thermal analysis (see Fig. 1.5).  $T_{1\rho}^H$  values can be obtained by fitting the decaying carbon resonance intensities of one's concern to the following exponential equation:

$$M(\tau) = M(0) \exp(-\tau/T_{1\rho}^H) \quad (2.2)$$

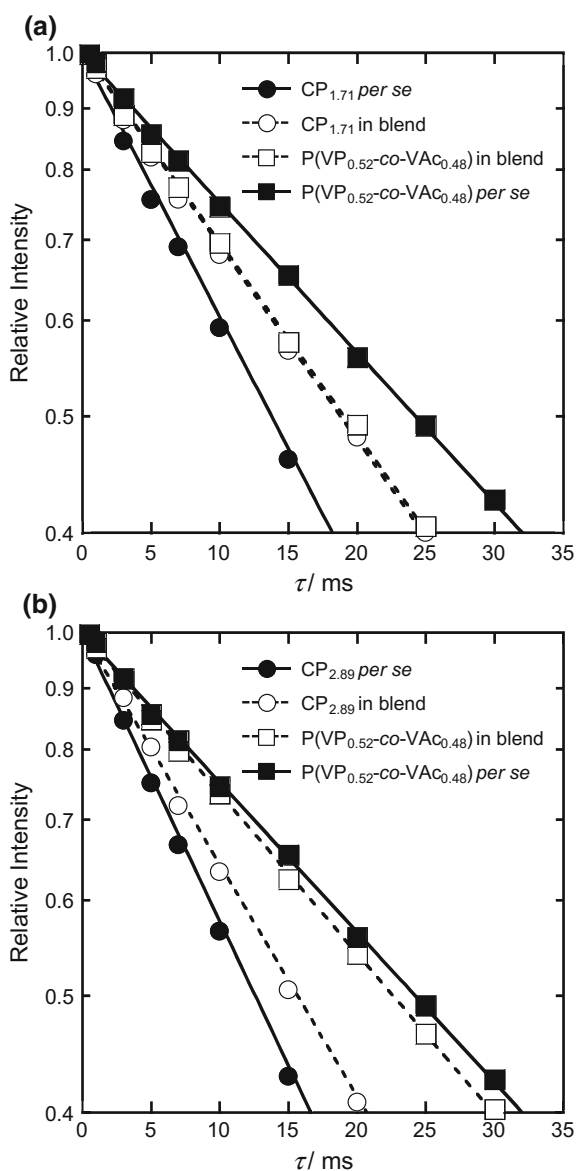
where  $M(\tau)$  is the magnetization intensity observed as a function of the spin-locking time  $\tau$ .

Figure 2.11 displays the decay behavior of  $^{13}\text{C}$  resonance intensities for two miscible blends of CP (DS = 1.71)/P(VP-*co*-VAc) (VP:VAc = 52:48) and CP (DS = 2.89)/P(VP-*co*-VAc) (VP:VAc = 52:48), the predominant factor contributory to the respective miscibility attainments being the intermolecular hydrogen-bonding for the former and the intramolecular repulsion in the copolymer for the latter [14]. Concerning the CP (DS = 1.71)/P(VP-*co*-VAc) blend (Fig. 2.11a),  $T_{1\rho}^H$  values of the two components coincide with each other just at the midpoint (27.9 ms) between the respective original values, 20.5 ms for the CP and 35.4 ms for the copolymer. Then, using the spin-diffusion equation, Eq. (1.3), the heterogeneity size  $L$  of this blend is estimated at  $L = \sim 4\text{ nm}$  as the maximum. Such an equalization of  $T_{1\rho}^H$ s of two components was exemplified for other miscible blends of hydrogen-bonding type, not only in the CP system but also in the CA and CB systems with P(VP-*co*-VAc) or P(VP-*co*-MMA) as a mixing partner [13, 15–17]. By additional spectroscopic evidence of the interaction, it has been ensured that those blends are homogeneous at the molecular segmental level of less than a few nanometers.

In the other example using the high-substituted CP/P(VP-*co*-VAc) blend (Fig. 2.11b), there arises a serious disagreement between  $T_{1\rho}^H$ s of the two polymer components; that is, the respective relaxation processes proceed almost independently, indicating less cooperative spin diffusion. A similar temporal disagreement was observed for other blends situated in the miscibility window in the CP/P(VP-*co*-VAc) map (Fig. 2.2b), and this was also the case for the CP/P(VP-*co*-MMA) (Fig. 2.5b) and CB/P(VP-*co*-VAc) systems (Fig. 2.2c). By combined use of the  $T_{1\rho}^H$  result and DSC data, it can be said that the scale of homogeneity in the miscible blends using highly substituted CP and CB lies between ca. 4 and 25 nm.



**Fig. 2.11** Semilogarithmic plots of the decay of  $^{13}\text{C}$  resonance intensities as a function of spin-locking time  $\tau$ , for solid films of **a** CP (DS = 1.71), P(VP-co-VAc) (VP:VAc = 52:48), and their 50/50 blend, and **b** CP (DS = 2.89), P(VP-co-VAc) (VP:VAc = 52:48), and their 50/50 blend (Reproduced with permission from [14])



### 2.2.3 Application to Functional Films

In this section, we illustrate significant applications of some selected CE/vinyl (co) polymer blends to functional films. After referring to a few examples of separation membrane using CE blends, our major concern is focused on oriented films mainly

of the miscible CA/P(VP-*co*-MMA) blends; this blend system has a high potential as an important optical element in the display field.

### (a) *Separation Membranes*

For further functional development of CEs as membrane materials, the improvement of their adsorption property in a broad sense, such as liquid- or vapor-permeation selectivity, is required. In relation to this, Nguyen et al. examined pervaporation characteristics of CA/P(VP-*co*-VAc) blends for application as alcohol-selective membrane materials [26, 27]. According to the study, through specific interactions of VP-carbonyls in the copolymer with ethanol, the blend membranes make efficient removal of ethanol from its mixture with ethyl *tert*-butyl ether (ETBE) that is an environmentally friendly octane-value enhancer for motor fuels. In the process of ETBE production, an excess of ethanol has to be separated from the reaction system and recycled. However, the conventional separation process by distillation is quite inefficient to the ethanol/ETBE mixtures, because ethanol forms an azeotropic mixture with ETBE. The CA/P(VP-*co*-VAc) pervaporation membrane may be a potential alternative to the conventional distillation method.

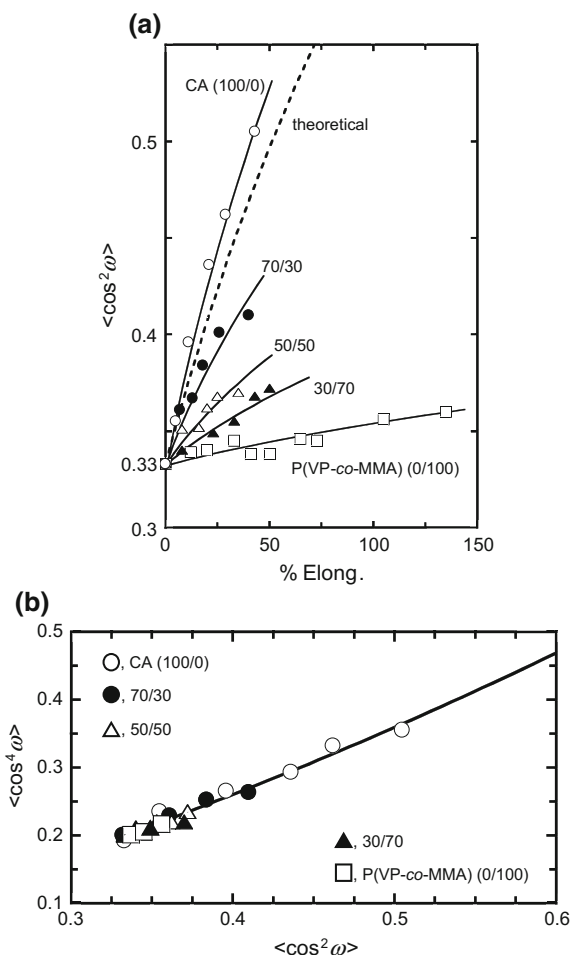
Concerning gas separation membranes, He, O<sub>2</sub>, and N<sub>2</sub> gas transport properties of compatible CA/PMMA blends have been measured [18]. According to this report, the blend films conditionally form a layered morphology with the surface layers rich in PMMA and the interior composed of the polymer mixture, and they show a high-selective permeability to He gas due to the unique morphology. Thus the CA/PMMA blends may be useful for a membrane material to produce a high-purity helium gas stream in a simple process.

### (b) *Optical Films*

In connection with the utility of CEs as optical films to regulate or modulate polarized light in modern displays, our attention has recently been directed to the molecular orientation and optical anisotropy invited by deformation of CE-based films [5, 28]. In an elaborate work by Ohno and Nishio [28], a fluorescence polarization technique [29, 30] was utilized to obtain information about the degree and type of molecular orientation in uniaxially drawn films of the miscible CA/P(VP-*co*-MMA) blends, each film containing a slight amount of a fluorescent probe, 4,4'-bis(2-benzoxazolyl)stilbene (see Fig. 1.7a in Chap. 1). Birefringence quantification was also carried out for the drawn films, in order to estimate the state of optical anisotropy induced therein.

In Fig. 2.12a, the second moment of molecular orientation,  $\langle \cos^2 \omega \rangle$ , defined in Sect. 1.4.2 of Chap. 1, is plotted against the percentage elongation of film specimens of CA (DS = 1.80)/P(VP-*co*-MMA) (VP = 35 mol%) blends. For all the blend compositions, we can see that the value of  $\langle \cos^2 \omega \rangle$  increases monotonically from 0.33 with increasing extent of elongation. Therefore, it follows that any of the drawn films imparts a “positive” orientation function, i.e.,  $f = (3\langle \cos^2 \omega \rangle - 1)/2 > 0$ , indicating a normal trend of molecular orientation in the draw direction. However, the development of orientation becomes suppressed with increasing

**Fig. 2.12** Plots of **a**  $\langle \cos^2 \omega \rangle$  versus % elongation and **b**  $\langle \cos^4 \omega \rangle$  versus  $\langle \cos^2 \omega \rangle$  for drawn blends of CA (DS = 1.80)/P(VP-co-MMA) (VP:MMA = 35:65). (Rearranged by using data from [28] and additional data, with permission)



content of the vinyl polymer component; the two constituent polymers would be oriented cooperatively in the miscible blend films during the course of the uniaxial drawing process (see below).

Figure 2.12b illustrates a plot of the fourth moment  $\langle \cos^4 \omega \rangle$  against the second moment  $\langle \cos^2 \omega \rangle$  of molecular orientation for the CA (DS = 1.80)/P(VP-co-MMA) (VP = 35 mol%) blends. All the data satisfactorily fit a relationship between the two moments calculated in terms of a prolate ellipsoidal model of orientation distribution; the relationship is virtually equivalent to a theoretical one predicted by a Kratky-type affine deformation scheme [31]. Thus the type of molecular orientation in the drawn blends always follows this orthodox model, although the rate of orientation development depends on the blend composition.

Meanwhile, birefringence of an oriented polymer film, which is defined as  $\Delta n = n_{\parallel} - n_{\perp}$  with a refractive index ( $n_{\parallel}$ ) parallel to the draw direction and that ( $n_{\perp}$ ) perpendicular to it, in general, varies with the degree of orientation, according to the equation:

$$\Delta n = \{ (3 \langle \cos^2 \omega_s \rangle - 1) \Delta n^{\circ} \} / 2 \quad (2.3)$$

where  $\Delta n^{\circ}$  is an intrinsic birefringence for the perfect uniaxial orientation of the polymer chains, and  $\langle \cos^2 \omega_s \rangle$  is the second moment of orientation for an anisotropic segmental unit  $S$  with a certain polarizability. Here it should be stressed that the two second moments,  $\langle \cos^2 \omega \rangle$  and  $\langle \cos^2 \omega_s \rangle$ , obtained from the fluorescence polarization and birefringence measurements, respectively, are different in magnitude from each other, because there is a respectable difference in size of the structural unit for orientation estimation between the two methods (see Fig. 2.13a).

Figure 2.14 compiles results of the birefringence measurements conducted for drawn films of three miscible series of CA/P(VP-*co*-MMA) blends prepared in different combinations of DS and VP:MMA ratio: (a) DS = 1.80 and VP:MMA = 35:65; (b) DS = 2.18 and VP:MMA = 47:53; and (c) DS = 2.48 and VP:MMA = 50:50. Drawn films of the vinyl copolymers show negative optical anisotropy ( $\Delta n^{\circ}_{\text{P(VP-co-MMA)}} < 0$ ), whereas the CAs (DS  $\leq 2.75$ ) exhibit positive optical anisotropy ( $\Delta n^{\circ}_{\text{CA}} > 0$ ) upon stretching of their films. Therefore, birefringence  $\Delta n$  of the blends is widely controllable in the degree and polarity, by altering the DS of CA, the VP:MMA ratio in P(VP-*co*-MMA), and the polymer composition of blending. With a certain specific blend composition, the drawn film can behave like an optically isotropic medium even though it should be mechanically anisotropic due to orientation development. The critical binary composition where the blend remains a birefringence-free material shifts to the CA-rich composition side with increasing DS of the CA used and with increasing VP fraction in the P(VP-*co*-MMA) component (see Fig. 2.13b). As seen in Fig. 2.14b, c, some blend films rich in the vinyl copolymer can provide a negative  $\Delta n$  larger in magnitude than that of the respective unblended vinyl copolymers. This is because the negative contribution of the P(VP-*co*-MMA) component becomes more intensely pronounced, as a result of the cooperative orientation through hydrogen-bonding interaction with the semi-rigid CA component having a high orientation ability (see Fig. 2.13c).

A wide variation in birefringence of oriented CP blends has also been attained, using miscible combinations of CP/P(VP-*co*-MMA) of hydrogen-bonding type [17]. For instance, drawn films of CP (DS = 2.09)/P(VP-*co*-MMA) (VP = 47 mol%) can provide much larger  $\Delta n$  values in CP-rich compositions, compared to the corresponding films using a comparable CA (DS = 2.18). As an example using cellulose mixed ester, Yamaguchi et al. have studied optical birefringence of partially miscible CAP/PVAc blends that offered transparent films [32]. A zero-birefringence

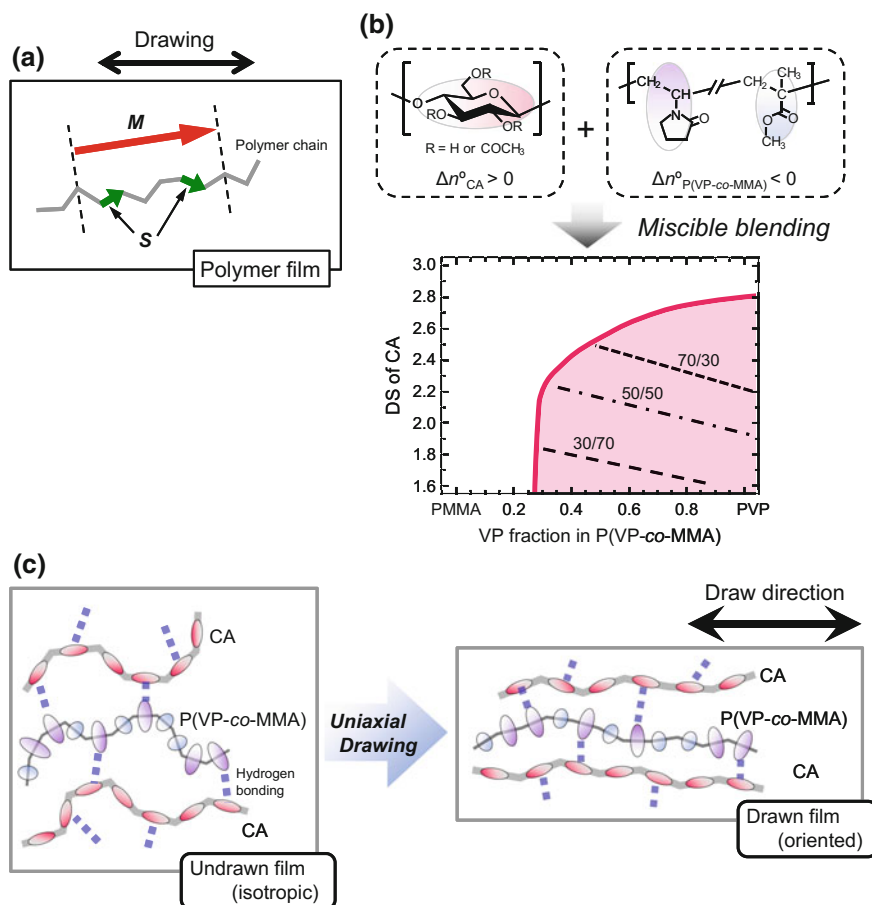


**Fig. 2.13** **a** Schematic representations of two structural units  $M$  (the molecular axis of a fluorescent probe with a length of  $\sim 2.5$  nm) and  $S$  (a statistical segment of shorter length, having a specific anisotropy in polarizability). **b** Miscibility map for CA/P(VP-co-MMA) blends with three dotted lines, designated as 70/30, 50/50, and 30/70, which inform a critical binary composition where a given polymer blend shows a zero-birefringence nature, irrespective of the draw ratio (Rearranged by using data from [28], with permission). **c** Schematic representation of molecular orientation induced in a film of CA/P(VP-co-MMA) upon uniaxial drawing. In **b** and **c**, polymer chains are illustrated in terms of a sequence of the polarizability ellipsoids of the constituent monomer units

phenomenon is realized for a film prepared at a composition of CAP: PVAc =  $\sim 50:50$ ; i.e., the drawn specimens exhibited no birefringence irrespective of the draw ratio.

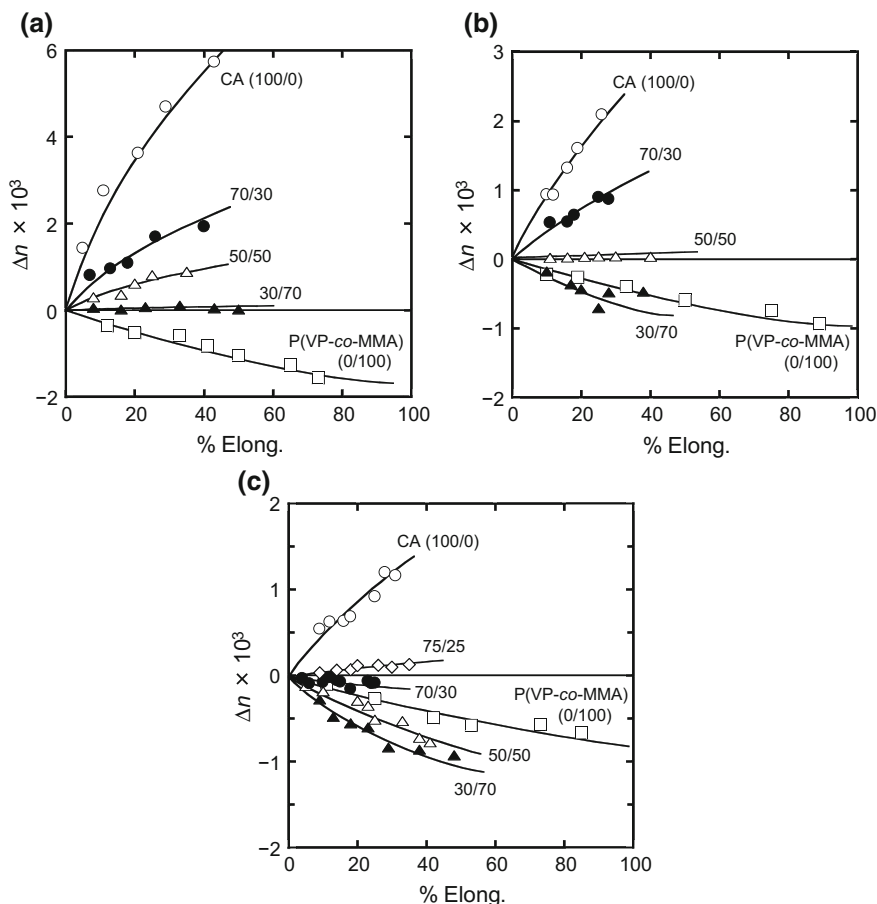


**Fig. 2.14** Birefringence  $\Delta n$  versus % elongation for drawn films of CA/P(VP-co-MMA) blends prepared at different combinations of DS and VP:MMA ratio: **a** DS = 1.80 and VP:MMA = 35:65; **b** DS = 2.18 and VP:MMA = 47:53; and **c** DS = 2.48 and VP/MMA = 50:50 (Reproduced with permission from [28])

### 2.3 Other Prominent Systems of Cellulose Ester/Vinyl Polymer Blend

In addition to the VP-containing vinyl (co)polymers employed above, a few hydrophilic vinyl polymers are known to be miscible with a couple of conventional CEs. There are several prominent studies on thermal and/or mechanical enhancements of the miscible blends by introducing intercomponent cross-links or inorganic clays therein, as summarized below. On the other hand, miscible blends of CEs with hydrophobic vinyl (homo)polymers are still rare. To attain their intimate mixing, however, there are some attempts to construct an interpenetrating polymer

network (IPN). This chemical technique is also a promising route to synergistically improve the thermal and mechanical performance and other physicochemical properties of cellulosic compositional materials.

### ***2.3.1 Enhancement of Thermomechanical Performance***

By the attainment of miscible blends of CE with amorphous vinyl polymers, the thermal (e.g.,  $T_g$ ), optical (e.g., orientation birefringence), and adsorption properties of CE can be improved, but the mechanical strength and heat resistance are often deteriorated. A remedy for such drawbacks in thermomechanical stability of the CE-based blends is introduction of chemical cross-linkages, as has been applied to a miscible CE/poly(vinyl phenol) (PVPh) system [33]; PVPh has potential for a secondary chemical reaction with cross-linking agent leading to the chain extension. This phenolic polymer is known to form miscible blends with a wide variety of polymers with hydrogen-bond accepting groups including commercially available CEs [34, 35]. Kelley et al. prepared polymer networks from miscible CA/PVPh and CAB/PVPh blends containing a latent formaldehyde source as cross-linker and showed improvement of the strength and thermal stability of the whole system [33].

Another method to effectively reinforce CE-based materials may be the use of layered clays as nano-filler [3, 36]. A recent successful example by the authors' group was nanoincorporation of various types of layered double hydroxides (LDHs) in a miscible blend of CA/poly(acryloyl morpholine) (PACMO) [37]. The LDHs were incorporated by solution blending of CA with a polymer/inorganic hybrid precursor prepared by polymerization of ACOMO monomer containing each LDH powder. Amphiphilically modified organophilic LDHs (LDH[M]) were well exfoliated and dispersed in the cast blend films; this gave rise to an excellent effect of thermomechanical reinforcement, which was assessed by dynamic mechanical analysis (see Fig. 2.15).

### ***2.3.2 Intimate Mixing of Cellulosic Blend by In Situ Polymerization of Vinyl Monomer***

As summarized in previous reviews [3, 38, 39], highly compatible blends are obtained for some pairs of unmodified cellulose/vinyl polymer, using a suitable non-aqueous solvent and procedure for each individual case. As a noteworthy act in the '90 s, Nishio and Miyashita proposed a new route leading to unique micro-composites of cellulose [40, 41]. In situ polymerization of vinyl monomers as coagulant and/or impregnant used to form cellulose gels is an essential part of the method. Thereby, it is possible to synthesize an IPN of cellulose/vinyl polymer, where the mixing level of the two polymers can be at a few nanometers, even though the pair is originally immiscible.

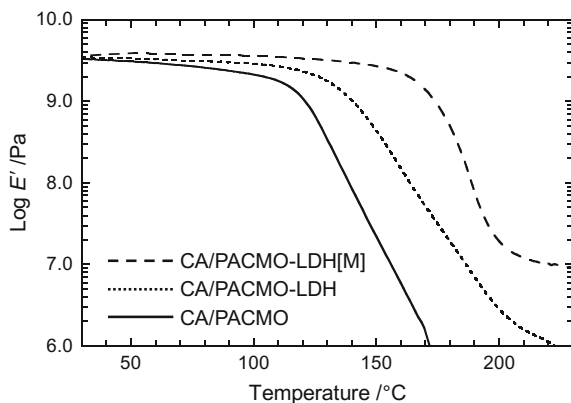


**Fig. 2.15** Temperature dependence of the dynamic storage modulus  $E'$  for CA/PACMO, CA/PACMO-LDH, and CA/PACMO-LDH[M] (Quoted with permission from [37]). Their polymer compositions were unified as CA/PACMO = 50/50 (wt/wt), and the content of LDH or LDH[M] was adjusted to  $\sim 3.2$  wt%. In this example, 12-hydroxyteric acid-modified LDH was used as LDH[M]

A similar technique of “in situ polymerization” is applicable to microscopic composition of CEs with vinyl polymers. Aoki et al. have successfully exemplified unique IPN composites made up of CA and PMMA [42]; the pair usually forms immiscible blends when prepared by simple solution-casting. An SH-containing CA was prepared in advance by additional esterification of CA with mercaptoacetic acid, and then the interpenetration and cross-linking between the polymer components were simultaneously attained by thiol–ene polymerization of MMA in solutions of the modified CA. The dried composites, belong to a joined type of IPN [3], exhibited a higher tensile strength and a better ductility in film form, without parallel in any film of CA, PMMA, and immiscible CA/PMMA blends.

## 2.4 Concluding Remarks

The present chapter surveyed recent studies on the blend miscibility of CEs mainly with vinyl copolymers comprising the VP unit. The estimation was conducted by DSC thermal analysis ( $T_g$  detection), and the results were represented in the miscibility maps as a function of DS of the CE component and VP fraction of the copolymer component. Through comparison between the maps, it was revealed that the miscibility behavior of the CEs with a given vinyl copolymer drastically changed depending on the carbon number of the acyl substituent of CE. In addition to the specific intermolecular interactions such as hydrogen bonding, the repulsive intra-copolymer effect played an important role for the miscibility attainment; the latter effect was embodied by the appearance of a “miscibility window” in the maps



for the CP and CB blend systems. Attractive or repulsive interactivities between the blend-constituting polymers were also evaluated in terms of the viscometric interaction parameter. Consequently, we were able to satisfactorily comprehend the miscibility behavior of the CE/VP-containing copolymer blends.

Besides the basic characterization, we reviewed some useful studies of miscible CE blends that showed remarkably improved adsorption, optical, or thermomechanical properties toward their possible functional development. In the representative example for the miscible CA/P(VP-*co*-MMA) system, the orientation birefringence of deformed blend films was proved to be widely controllable. The result demonstrating a synergistic effect in optical property of the CE-based blends provides a suggestive idea to develop new optical media using cellulose in the future.

## References

1. Edgar KJ, Buchanan CM, Debenham JS, Rundquist PA, Seiler BD, Shelton MC, Tindall D (2001) Advances in cellulose ester performance and application. *Prog Polym Sci* 26: 1605–1688. doi:[10.1016/S0079-6700\(01\)00027-2](https://doi.org/10.1016/S0079-6700(01)00027-2)
2. Rustemeyer P (ed) (2004) Cellulose acetates: properties and applications. Wiley-VCH, Weinheim
3. Nishio Y (2006) Material functionalization of cellulose and related polysaccharides via diverse microcompositions. *Adv Polym Sci* 205:97–151. doi:[10.1007/12\\_095](https://doi.org/10.1007/12_095)
4. Teramoto Y (2015) Functional thermoplastic materials from derivatives of cellulose and related structural polysaccharides. *Molecules* 20:5487–5527. doi:[10.3390/molecules20045487](https://doi.org/10.3390/molecules20045487)
5. Sugimura K, Teramoto Y, Nishio Y (2015) Cellulose acetate. In: Kobayashi S, Müllen K (eds) *Encyclopedia of polymeric nanomaterials*. Springer, Berlin/Heidelberg, pp 339–347
6. Paul DR, Newman S (eds) (1978) *Polymer blends*, vols 1 & 2. Academic Press, New York
7. Olabisi O, Robeson LM, Shaw MT (1979) *Polymer–polymer miscibility*. Academic Press, New York
8. Utracki LA (1990) *Polymer alloys and blends: thermodynamics and rheology*. Hanser, Munich/New York
9. Coleman MM, Graf JF, Painter PC (1991) Specific interactions and the miscibility of polymer blends: practical guides for predicting & designing miscible polymer mixtures. Technomic Pub., Lancaster
10. Masson J-F, Manley RSJ (1991) Miscible blends of cellulose and poly(vinylpyrrolidone). *Macromolecules* 24:6670–6679. doi:[10.1021/ma00025a018](https://doi.org/10.1021/ma00025a018)
11. Miyashita Y, Kimura N, Nishio Y, Suzuki H (1994) Transition behavior and phase structure of cellulose/poly(*N*-vinylpyrrolidone) composites prepared by a solution coagulation/bulk polymerization method. *Kobunshi Ronbunshu* 51:466–471. doi:[10.1295/koron.51.466](https://doi.org/10.1295/koron.51.466)
12. Miyashita Y, Suzuki T, Nishio Y (2002) Miscibility of cellulose acetate with vinyl polymers. *Cellulose* 9:215–223. doi:[10.1023/A:1021144827845](https://doi.org/10.1023/A:1021144827845)
13. Ohno T, Yoshizawa S, Miyashita Y, Nishio Y (2005) Interaction and scale of mixing in cellulose acetate/poly(*N*-vinyl pyrrolidone-*co*-vinyl acetate) blends. *Cellulose* 12:281–291. doi:[10.1007/s10570-004-5836-7](https://doi.org/10.1007/s10570-004-5836-7)
14. Sugimura K, Katano S, Teramoto Y, Nishio Y (2013) Cellulose propionate/poly(*N*-vinyl pyrrolidone-*co*-vinyl acetate) blends: dependence of the miscibility on propionyl DS and copolymer composition. *Cellulose* 20:239–252. doi:[10.1007/s10570-012-9797-y](https://doi.org/10.1007/s10570-012-9797-y)

15. Ohno T, Nishio Y (2006) Cellulose alkyl ester/vinyl polymer blends: effects of butyryl substitution and intramolecular copolymer composition on the miscibility. *Cellulose* 13: 245–259. doi:[10.1007/s10570-005-9014-3](https://doi.org/10.1007/s10570-005-9014-3)
16. Ohno T, Nishio Y (2007) Estimation of miscibility and interaction for cellulose acetate and butyrate blends with *N*-vinylpyrrolidone copolymers. *Macromol Chem Phys* 208:622–634. doi:[10.1002/macp.200600510](https://doi.org/10.1002/macp.200600510)
17. Sugimura K, Teramoto Y, Nishio Y (2013) Blend miscibility of cellulose propionate with poly(*N*-vinyl pyrrolidone-*co*-methyl methacrylate). *Carbohydr Polym* 98:532–541. doi:[10.1016/j.carbpol.2013.06.045](https://doi.org/10.1016/j.carbpol.2013.06.045)
18. Bikson B, Nelson JK, Muruganandam N (1994) Composite cellulose acetate/poly(methyl methacrylate) blend gas separation membranes. *J Membr Sci* 94:313–328. doi:[10.1016/0376-7388\(94\)87041-1](https://doi.org/10.1016/0376-7388(94)87041-1)
19. Sugimura K, Teramoto Y, Nishio Y (2015) Insight into miscibility behaviour of cellulose ester blends with *N*-vinyl pyrrolidone copolymers in terms of viscometric interaction parameters. *Cellulose* 22:2349–2363. doi:[10.1007/s10570-015-0660-9](https://doi.org/10.1007/s10570-015-0660-9)
20. Krigbaum WR, Wall FT (1950) Viscosities of binary polymeric mixtures. *J Polym Sci* 5: 505–514. doi:[10.1002/pol.1950.120050408](https://doi.org/10.1002/pol.1950.120050408)
21. Cragg LH, Bigelow CC (1955) The viscosity slope constant  $k'$ —ternary systems: polymer–polymer–solvent. *J Polym Sci* 16:177–191. doi:[10.1002/pol.1955.120168208](https://doi.org/10.1002/pol.1955.120168208)
22. Chee KK (1990) Determination of polymer–polymer miscibility by viscometry. *Eur Polym J* 26:423–426. doi:[10.1016/0014-3057\(90\)90044-5](https://doi.org/10.1016/0014-3057(90)90044-5)
23. MacBrierty VJ, Douglass DC (1981) Recent advances in the NMR of solid polymers. *J Polym Sci Macromol Rev* 16:295–366. doi:[10.1002/pol.1981.230160105](https://doi.org/10.1002/pol.1981.230160105)
24. Masson J-F, Manley RSJ (1992) Solid-state NMR of some cellulose/synthetic polymer blends. *Macromolecules* 25:589–592. doi:[10.1021/ma00028a016](https://doi.org/10.1021/ma00028a016)
25. Miyashita Y, Kimura N, Suzuki H, Nishio Y (1998) Cellulose/poly(acryloyl morpholine) composites: synthesis by solution coagulation/bulk polymerization and analysis of phase structure. *Cellulose* 5:123–134. doi:[10.1023/A:1009224931504](https://doi.org/10.1023/A:1009224931504)
26. Nguyen QT, Noezar I, Clément R, Streicher C, Brueschke H (1997) Poly(vinyl pyrrolidone-*co*-vinyl acetate)–cellulose acetate blends as novel pervaporation membranes for ethanol–ethyl tert-butyl ether separation. *Polym Adv Technol* 8:477–486. doi:[10.1002/\(SICI\)1099-1581\(199708\)8:8<477::AID-PAT653>3.0.CO;2-0](https://doi.org/10.1002/(SICI)1099-1581(199708)8:8<477::AID-PAT653>3.0.CO;2-0)
27. Nguyen QT, Clément R, Noezar I, Lochon P (1998) Performances of poly(vinylpyrrolidone-*co*-vinyl acetate)–cellulose acetate blend membranes in the pervaporation of ethanol–ethyl tert-butyl ether mixtures: simplified model for flux prediction. *Sep Purif Technol* 13:237–245. doi:[10.1016/S1383-5866\(98\)00046-X](https://doi.org/10.1016/S1383-5866(98)00046-X)
28. Ohno T, Nishio Y (2007) Molecular orientation and optical anisotropy in drawn films of miscible blends composed of cellulose acetate and poly(*N*-vinylpyrrolidone-*co*-methyl methacrylate). *Macromolecules* 40:3468–3476. doi:[10.1021/ma062920t](https://doi.org/10.1021/ma062920t)
29. Nishijima Y (1970) Fluorescence methods in polymer science. *J Polym Sci Part C Polym Symp* 31:353–373. doi:[10.1002/polc.5070310128](https://doi.org/10.1002/polc.5070310128)
30. Nishio Y, Suzuki H, Sato K (1994) Molecular orientation and optical anisotropy induced by the stretching of poly(vinyl alcohol)/poly(*N*-vinyl pyrrolidone) blends. *Polymer* 35: 1452–1461. doi:[10.1016/0032-3861\(94\)90345-X](https://doi.org/10.1016/0032-3861(94)90345-X)
31. Kratky O (1933) Zum deformationsmechanismus der faserstoffe, I (On the deformation mechanism of the fiber, I). *Kolloid-Z* 64:213–222. doi:[10.1007/BF01434162](https://doi.org/10.1007/BF01434162)
32. Yamaguchi M, Masuzawa K (2007) Birefringence control for binary blends of cellulose acetate propionate and poly(vinyl acetate). *Eur Polym J* 43:3277–3282. doi:[10.1016/j.eurpolymj.2007.06.007](https://doi.org/10.1016/j.eurpolymj.2007.06.007)
33. Gaibler DW, Rochefort WE, Wilson JB, Kelley SS (2004) Blends of cellulose ester/phenolic polymers—chemical and thermal properties of blends with polyvinyl phenol. *Cellulose* 11:225–237. doi:[10.1023/B:CELL.0000025425.00668.de](https://doi.org/10.1023/B:CELL.0000025425.00668.de)

34. Landry MR, Massa DJ, Landry CJT, Teegarden DM, Colby RH, Long TE, Henrichs PM (1994) A survey of polyvinylphenol blend miscibility. *J Appl Polym Sci* 54:991–1011. doi:[10.1002/app.1994.070540801](https://doi.org/10.1002/app.1994.070540801)
35. Davis MF, Wang XM, Myers MD, Iwamiya JH, Kelley SS (1998) A study of the molecular interactions occurring in blends of cellulose esters and phenolic polymers, chap. 20. In: Heinze TJ, Glasser WG (eds) *Cellulose derivatives: modification, characterization, and nanostructures*. (ACS Symp Ser vol. 688) American Chemical Society, Washington DC
36. Park HM, Misra M, Drzal LT, Mohanty AK (2004) “Green” nanocomposites from cellulose acetate bioplastic and clay: effect of eco-friendly triethyl citrate plasticizer. *Biomacromolecules* 5:2281–2288. doi:[10.1021/bm049690f](https://doi.org/10.1021/bm049690f)
37. Yoshitake S, Suzuki T, Miyashita Y, Aoki D, Teramoto Y, Nishio Y (2013) Nanoincorporation of layered double hydroxides into a miscible blend system of cellulose acetate with poly(acryloyl morpholine). *Carbohydr Polym* 93:331–338. doi:[10.1016/j.carbpol.2012.03.036](https://doi.org/10.1016/j.carbpol.2012.03.036)
38. Nishio Y (1994) Hyperfine composites of cellulose with synthetic polymers, chap. 5. In: Gilbert RD (ed) *Cellulosic polymers, blends and composites*. Carl Hanser, Munich
39. Vigo TL (1998) Interaction of cellulose with other polymers: retrospective and prospective. *Polym Adv Technol* 9:539–548. doi:[10.1002/\(SICI\)1099-1581\(199809\)9:9<539::AID-PAT813>3.0.CO;2-I](https://doi.org/10.1002/(SICI)1099-1581(199809)9:9<539::AID-PAT813>3.0.CO;2-I)
40. Miyashita Y, Nishio Y, Kimura N, Suzuki H, Iwata M (1996) Transition behaviour of cellulose/poly(*N*-vinylpyrrolidone-*co*-glycidyl methacrylate) composites synthesized by a solution coagulation/bulk polymerization method. *Polymer* 37:1949–1957. doi:[10.1016/0032-3861\(96\)87313-7](https://doi.org/10.1016/0032-3861(96)87313-7)
41. Miyashita Y, Yamada Y, Kimura N, Suzuki H, Iwata M, Nishio Y (1997) Phase structure of chitin/poly(glycidyl methacrylate) composites synthesized by a solution coagulation/bulk polymerization method. *Polymer* 38:6181–6187. doi:[10.1016/S0032-3861\(97\)00174-2](https://doi.org/10.1016/S0032-3861(97)00174-2)
42. Aoki D, Teramoto Y, Nishio Y (2011) Cellulose acetate/poly(methyl methacrylate) interpenetrating networks: synthesis and estimation of thermal and mechanical properties. *Cellulose* 18:1441–1454. doi:[10.1007/s10570-011-9580-5](https://doi.org/10.1007/s10570-011-9580-5)

Blends and Graft Copolymers of Cellulosics  
Toward the Design and Development of Advanced Films  
and Fibers

Nishio, Y.; Teramoto, Y.; Kusumi, R.; Sugimura, K.;  
Aranishi, Y.

2017, XIII, 125 p. 71 illus., Softcover

ISBN: 978-3-319-55320-7